Green hydrogen Production from the oxidative reform of clean biogas over Ni/MgO-Nb_2O_5 catalysts

Yvan J. O. Asencios, Elisabete M. Assaf

Y.J.O. Asencios, Institute of Marine Sciences, Federal University of São Paulo (UNIFESP), R. Maria Máximo 168, Santos 11030-100, SP, Brazil (e-mail: yvan.jesus@unifesp.br); Center for Natural Sciences and Humanities, Federal University of ABC (UFABC), Av. dos Estados 5001, Santo André 09210-580, SP, Brazil. E.M.Assaf, São Carlos Institute of Chemistry, University of Sao Paulo (USP), Av. Trabalhador São Carlense 400, Brazil (e-mail: eassaf@iqsc.usp.br)

DOI: https://doi.org/10.34024/jsse.2023.v1.15904

***Abstract*—Synthesis gas has a variety of applications ranging from its transformation into Fischer-Tropsch fuels, its processing to produce pure hydrogen, and even its direct combustion to generate energy, among many other applications. The objective of this work was the conversion of a model of biogas (clean biogas) into synthesis gas, H_2 /CO, through oxidative reforming of methane over NiO/MgO/Nb_2O_5 catalysts. The catalysts in this work were prepared by impregnation and calcination (at 750°C) and subsequently characterized by Energy Dispersive X-ray spectroscopy (EDX), Scanning Electron Microscopy (SEM), X-ray diffraction (XRD), Nitrogen Adsorption-Desorption (BET method) and Temperature Programmed Reduction with H2 (TPR). Finally, these catalysts were tested in the oxidative reform of methane (molar ratio of 1.5CH_4:1CO_2:0.25O_2) at 750 °C, 100mg of catalyst at a total flow of 110 mL.min^{-1}, and 1 atm (inside the reactor). According to the results, it was verified that the catalyst composed of the NiO/MgO mixture is composed of the NiO-MgO solid solution, whereas the NiO/MgO/Nb_2O_5 catalysts are also formed by nickel niobate ($NiNb_2O_6$). All catalysts showed catalytic activity in the oxidative form of biogas, NiMg, Ni60NbMg, and Ni40NbMg catalysts showed the highest conversion value. The efficiency of the catalysts in the oxidative reforming of biogas improved gradually as the %MgO increased in the NiO/MgO/Nb_2O_5 system. The characterization of the catalyst after the reaction demonstrated that the carbon formed is of the filamentous type.**

***Keywords*: methane, biogas, synthesis gas, catalysts, nickel, niobium.**

I. Introduction

Hydrogen is considered the fuel of the future in the medium and long term, as its use as an energy source can help reduce the emission of greenhouse gases such as CO_2, thus avoiding global warming and thereby mitigating the climate changes that damage the planet Earth. It is known that hydrogen is abundant on planet Earth, as it is found forming water molecules (H_2O) and organic molecules (for example in oil, natural gas, and many any organic matter, etc.), obtaining hydrogen in pure form requires chemical processes and demands high energy consumption.

Although hydrogen has no color, green hydrogen (also called renewable hydrogen) is defined as hydrogen that is produced from a renewable resource and a renewable energy source. Brazil is a strategic country to produce green hydrogen, given its clean electrical matrix, based almost entirely on renewable energies (mainly hydroelectric, wind, and solar). There are several ways to produce green hydrogen, for example from the alkaline electrolysis of water using electricity from renewable sources (for example: coming from water, solar, wind, etc.).

Biogas is significant for the society of today, as it is a clean source of energy and is considered a renewable biofuel. Biogas is produced by anaerobic fermentation of biomass, its main components are carbon dioxide and methane [1]. One way (but not the only one) to produce green hydrogen from biogas, is through reforming reactions, in which the energy needed for this process comes from renewable sources. The process consists of converting biogas into synthesis gas (a gaseous mixture of H_2/CO, also called Syngas) through the oxidative reform of methane, which occurs through the following overall reaction (reaction 1):

$$ORM: 1.5CH_4 + CO_2 + 0.25O_2 \rightarrow 2.5CO + 3H_2 \quad \Delta H^0_{298K} = 249.2\ kJ.mol^{-1} \qquad (1)$$

Reaction 1 considers the main components of biogas in a composition of 1.5CH_4/1CO_2, and to be carried out, it needs clean biogas, which means free of components usually found in raw biogas such as NH_3 and H_2S, which are detrimental to reform catalysts. Biogas reforming has been studied previously with excellent results [2]–[4].

Syngas can then go through the Water-Gas Shift reaction (WGSR, to give a mixture of H_2 and CO_2) and subsequently undergo an absorption process (with amines to remove CO_2) to purify hydrogen, which can be used by industry for several applications, it can also even be used as fuel in fuel cells. [5].

The advantage of converting biogas into Syngas goes beyond the production of hydrogen, as Syngas can be converted into liquid fuels by the Fischer-Tropsch process (or the so-called Gas-To-Liquid Process) [6]. Also, Syngas can be used directly as fuel in some types of engines, among other applications.

Group VIII B metals (e.g., Pt, Pd, Rh, Ru, and Ni) have been

used in methane reforming studies. The catalyst based on Ni supported on alumina, is used by the industry (which produces hydrogen from natural gas, through steam reforming of methane), owing to its good catalytic activity and its low cost (when compared to noble metals) [4]. However, nickel catalysts favor the formation and deposition of coke on the catalyst, this process is inevitable since the initial step of methane reform is the formation of carbon. Excessive coke deposition can lead to catalyst deactivation, reactor clogging, and even explosion. In this sense, several strategies have been applied to reduce these problems, among them: changing the composition of the catalytic support, adding promoter metals, and synthesizing catalytic metal nanoparticles, among others.

NiO-MgO solid solution has been used as a catalyst in biomethane and biogas reforming reactions showing excellent reagent conversion values, however, it presents high rates of carbon deposition [7]–[10].

Brazil holds the largest niobium reserve in the world and is the largest producer, representing 98% of world production [[11]], which makes it attractive to find new applications and enable its use for the benefit of science and society. Its use in catalysis is still recent. According to the Scopus database, by using the keywords: "niobium" and "catalysts", until the moment of publication of this article, there are 3,519.00 articles produced on this topic, the first of which was in 1973, and from 2000, scientific production has been growing exponentially. According to the same database, scientific production of niobium is led by China, the United States, Japan, Brazil, and India (in that descending order). Niobium application for methane reforming reactions is still scarce.

Nb_2O_5 is an acidic solid, with redox properties, it presents photocatalytic activity and intermediate surface area. The Nb_2O_5 is not much explored in methane reforming reactions, possibly the acidic properties that may favor high rates of carbon formation. In this work the mixture of three oxides was studied: NiO, MgO, and Nb_2O_5. The NiO/MgO catalyst is widely known as mentioned earlier, and the presence of MgO could decrease the acidity of Nb_2O_5, and new catalytic properties could be formed in this catalyst. This work explores the catalytic behavior of Nickel catalysts supported on different mixtures of MgO/Nb_2O_5 (containing different Mg/Nb ratios) in the biogas oxidative reforming reaction to produce Syngas.

II. MATERIALS AND METHODS

2.1 Preparation of NiO/MgO/Nb_2O_5 catalysts

Firstly, Nb_2O_5/MgO catalytic supports were prepared. For this procedure, magnesium oxide (MgO, 99.9% p.a.) was impregnated on the Nb_2O_5 using distilled water as a solvent, using a rotary evaporator. Nb_2O_5 was previously obtained according to the procedure detailed in Ferraz et al. [2018]. The used mass ratios of Nb_2O_5:MgO were: 0:100, 10:90, 40:60, 60:40, and 100:0. The mixtures obtained from the impregnation method were subsequently dried at 100°C and calcined at 750°C for 2 hours in an airflow of 30 ml.min^{-1}. These catalytic supports obtained were later impregnated with hydrated nickel nitrate $Ni(NO_3)_2.6H_2O$ (99.99%, Alfa-Aesar), at a nickel percentage of 10% (% total mass of catalyst) for each sample. The final calcination was carried out for three hours in an airflow of 30 ml.min^{-1} at 750ºC, for the formation of NiO (supported on Nb_2O_5/MgO). The catalysts were named according to the % of Nb in the composition: NiMg, Ni10NbMg, Ni40NbMg, Ni60NbMg, and NiNb, all catalysts have 10% Nickel (total mass of catalyst). NiNb and NiMg correspond to 100% and 0% of Nb, respectively.

Characterization of the catalysts

The catalysts were characterized by X-ray diffraction analysis (XRD) using a Rigaku Multiflex diffractometer (30kV,10mA), in the Bragg angle (2θ) range of 5 - 80º (and speed of 2°.min $^{-1}$) using Cu-K α radiation (λ = 1.5406Å). The XRD diffraction patterns were identified by comparison with the International Centre for Diffraction Data (JCPDS).

Temperature programmed reduction analyses (H_2-TPR) were carried out with 100mg of catalyst, using a gas mixture of 1.96 % H_2/Ar, flowing at 30 mL.min $^{-1}$, and a heating rate of 5°C min^{-1}, up to 1000ºC. The surface area measurements were performed on Quantachrome Nova 1200 equipment, and the results of nitrogen adsorption were treated according to the BET method.

Scanning electron microscopy with energy-dispersive X-ray spectroscopy (SEM/EDX) was used to study the morphology of the catalysts, and to quantify their chemical compositions. For this analysis, a small amount of the fresh catalyst was placed in isopropyl alcohol, forming a heterogeneous suspension. The suspension was dropped slowly onto a sample holder (of aluminum) aiming to disperse the powder catalyst. The SEM/EDX consists of a LEO-440 electron microscope with an Oxford detector, operating at a 20 kV electron beam. Before each analysis, the samples were sputter-coated with gold. For EDX analysis, 5 regions of the catalysts were selected, and the results of the chemical composition presented in this paper are the average values.

Catalytic tests of Oxidative Reform of Biogas

The catalytic tests were carried out in a fixed-bed down-flow reactor (a quartz reactor with an internal diameter = 10 mm). For each catalytic test, 100 mg of catalyst was used. Before each test, the catalyst was reduced with H_2 (99.9%, 30 mL.min^{-1}) for 1 hour, at 800°C. After that, the catalyst was then brought to the reaction temperature (750ºC) under pure N_2 flow.

In the Oxidative Reforming of Methane (ORM): the feed was a mixture of gases (60% CH_4 and 40% CO_2) and synthetic air

(O_2: 21%, N_2: 79%). The inlet gases reached a molar ratio of $1.5CH_4$:$1CO_2$:$0.25O_2$; giving a total flow of 107 mL.min^{-1}, inside the reactor. The reaction temperature was controlled and measured by a thermocouple inserted into the top of the catalyst bed.

The conversion % of CH_4 and CO_2 were calculated by the following equation:

$$R_{conversion}\,(\%) = \frac{R_{in} - R_{out}}{R_{in}} \times 100$$

where R is the molar flow rate (mol.min^{-1}) of CH_4 or CO_2.

The selectivity was calculated as:

$$Selectivity_{Ri} = \frac{R_{i\ produced}}{R_{CH4\ converted} + R_{CO2\ converted}} \times 100$$

where "R_i" is the molar flow rate (mol. min^{-1}) of the product (H_2 or CO).

Carbon deposition rate (mmol.C.h^{-1}) was determined as the apparent gain in mass of the catalyst after each reaction.

The unreacted reactants and gaseous products were analyzed in line with the catalytic unit test using a gas chromatograph (Varian, Model 3800). The chromatograph included two thermal conductivity detectors (TCD) and two columns; a 13X molecular sieve-packed column (that analyses H_2 using N_2 as a carrier), and a Porapak N column (that analyses CH_4, CO_2, and CO, using He as a carrier).

III. RESULTS AND DISCUSSIONS

Characterization of calcined catalysts, before the reaction: Elemental chemical analysis by EDX and Surface Area (S_{BET})

Table 1 presents the calculated theoretical values and the values obtained in the EDX analysis (average values) of the atomic composition of the catalysts, and the weight percentage of nickel. It can be seen that the values obtained through the EDX analysis are very close to the theoretical values, the desired percentage of Nickel in weight was 10% of total mass, however, the values obtained by EDX are close, and the small variations are due to experimental errors during preparation (example: weighing).

The surface area values (m^2.g^{-1}) are also in Table 1. The surface area values show a continuous decrease as Nb_2O_5 content increased in the mixture, this is probably due to the low surface area related to Nb_2O_5; the surface area value of the NiNb catalyst, which contains NiO/Nb_2O_5 was the lowest recorded.

Table 1. Elemental composition obtained by EDX analysis of the catalyst oxides, and surface area values obtained by the BET method.

	wt %	% Atomic (Theoretical)			% Atomic (EDX)			BET area (m^2.g^{-1})
Catalyst	Ni	Ni	Mg	Nb	Ni	Mg	Nb	
NiMg	10	11.89	88.11	0	10.56	89.44	0	40
Ni10NbMg	10	12.66	84.49	2.85	10.75	76.58	12.67	37
Ni40NbMg	13	15.76	70.08	14.17	16.16	62.74	21.1	33
Ni60NbMg	12	18.82	55.8	25.38	20.69	58.93	20.38	30
NiNb	12	30.79	0	69.21	28.87	0	71.13	20

XRD analysis

Fig. 1a presents the XRD patterns of the catalysts, it can be seen that the NiMg catalyst formed a single crystalline phase of NiO-MgO solid solution (NiO: JCPDS 78-0643 and MgO: JCPDS 78-0430). The formation of this solid solution is explained by the fact that NiO and MgO have a face-centered cubic structure (or called FCC), they have similar lattice parameter values (4.19 Å and 4.21 Å for NiO and MgO, respectively), very similar bond lengths (2.10 Å and 2.11 Å for NiO and MgO, respectively) and identical ionic charges (Ni^{2+} e Mg^{2+}) [12]–[14].

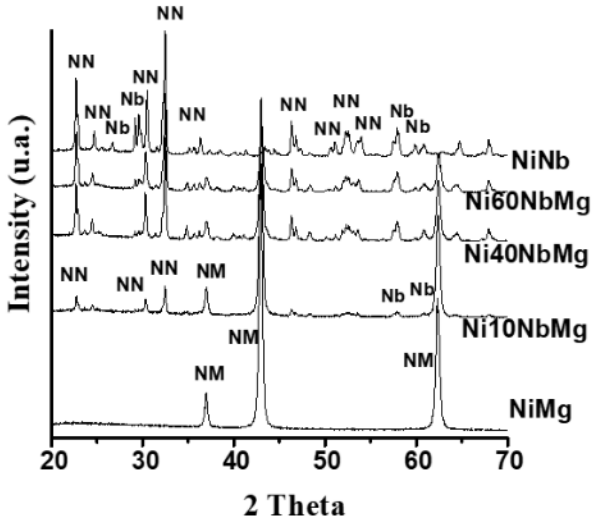

Figure 1a. XRD patterns of catalyst oxides, superposition of patterns. Caption: NiO:NiO; NM: NiO-MgO solid solution; Nb: Nb_2O_5; NN: nickel niobate $NiNb_2O_6$.

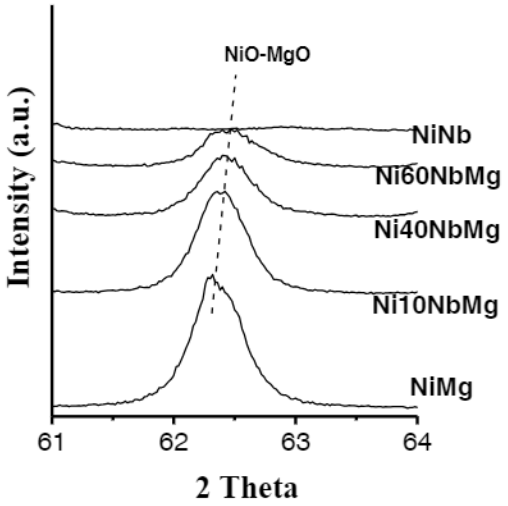

Figure 1b. Amplification between angles 61°-64° of the XRD patterns of catalysts. Caption: NiO: NiO; NM: NiO-MgO solid solution; Nb: Nb_2O_5; NN: nickel niobate $NiNb_2O_6$.

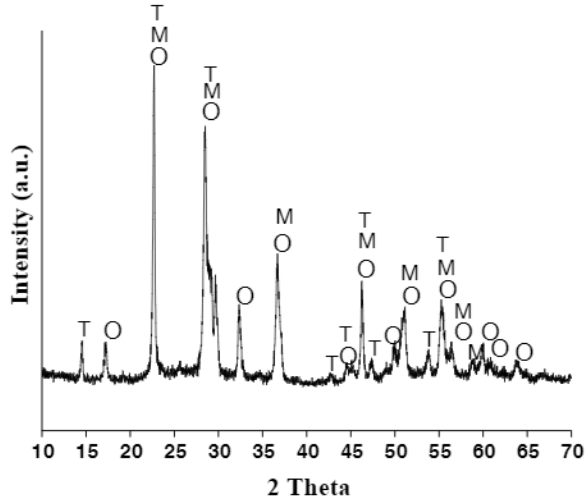

Figure 1c. XRD pattern of pure Nb_2O_5 pure. Caption: T: tetragonal phase; O: orthorhombic phase; M: monoclinic phase of Nb_2O_5

Figure 1b shows that there is a continuous displacement of the main peak of NiO (or NiO-MgO) towards larger Bragg angles, indicating a contraction in the lattice parameter. This contraction would indicate that Ni^{2+} ions entered the crystal lattice of MgO replacing some Mg^{2+} ions; as an effect of the formation of the NiO-MgO solid solution, a fact that would be reasonable since the ionic radius of Ni^{2+} (0.55 Å) is slightly smaller than that of Mg^{2+} (0.57Å) [5], [12], [15]. Upon these results, it is possible to affirm that this solid solution was formed in all samples that contain the three oxides: $NiO/MgO/Nb_2O_5$ since the displacement of the main peak of NiO is present in the XRD pattern of all these samples.

In the NiNb catalyst, a single phase of nickel niobate was observed ($NiNb_2O_6$ orthorhombic, JCPDS 15-159 and JCPDS 76-2354), indicating that the thermal condition during calcination at 750ºC in the presence of air favored the reaction between the two solid oxides (NiO and Nb_2O_5) leading to the formation of a single crystalline phase of nickel niobate. The structure of nickel niobate was also found by Kunimori et al [16], Guochang et al [17], and Cruz et al [18] using other synthesis methods.

In Figure 1a, in XRD patterns of the catalysts that contain the three oxides, it is observed that the peaks attributed to the $NiNb_2O_6$ crystalline phase become more intense as the content of Nb_2O_5 increases in the mixture. On the other hand, it is observed that at higher Nb_2O_5 content, the peaks corresponding to solid NiO-MgO solution become less intense. These findings indicate that when the three oxides ($NiO/MgO/Nb_2O_5$) are mixed, NiO gives rise to the two solid solutions: NiO-MgO and $NiNb_2O_6$; it seems that the growth of large crystallites of $NiNb_2O_6$ (represented by thinner and more intense XRD peaks) inhibit the formation of large structures in the NiO-MgO solid solution (expressed by less intense and wider peaks observed in Fig. 1).

The monoclinic crystalline phase of the Nb_2O_5 (Fig. 1a) was found in a low proportion (low-intensity peaks) only in the sample with 60% Nb_2O_5 (sample Ni60NbMg). The presence of $NiNb_2O_6$ becomes important because its reduction with H_2 (before the catalytic test) forms Niº with a strong metal-support interaction, which is essential to obtain a good catalytic activity [16]. There are two main advantages of using double oxides as catalysts (in this case $NiNb_2O_6$), the first is that its reduction leads to a high dispersion of Niº crystallites (which is beneficial for catalysis); the second is that in the case of Niº oxidation (for example by deactivation), $NiNb_2O_6$ can be recovered by calcination in the presence of air.

Figure 1c shows the XRD pattern of pure niobium oxide synthesized according to the methods explained in the previous section. This XRD pattern shows a mixture of Nb_2O_5 in tetragonal (JCPDS 18-911), monoclinic (JCPDS 27-1312), and orthorhombic crystalline phase (JCPDS 27-1313).

H_2-TPR

The reduction profiles of the oxide catalysts obtained by H_2-TPR analysis are shown in Figure 2. Figure 2 shows the reduction profiles of catalysts and Nb_2O_5, obtained by H_2-TPR analysis. Because the Nb_2O_5 did not show a significant reduction peak in the temperature range studied, all reduction peaks observed in the catalyst profiles were attributed to the reduction of Ni^{2+} present in the catalysts. The reduction profile of the NiNb sample represents the reduction of Ni^{2+} present in the $NiNb_2O_6$ structure (this crystalline structure was previously confirmed in XRD). This reduction profile indicates that Ni^{2+} stabilization in $NiNb_2O_6$ structure is weak, probably due to the high electronegativity of Nb^{5+} (=1.862) compared to Ni^{2+} (=1.367), which leads to high polarization of the Ni-O bond in the crystal lattice of $NiNb_2O_6$, and which consequently leads to a high reduction of Ni^{2+} [19]. The H_2-TPR profile of the NiNb sample is very similar to that found by Faro et al.[20] for nickel niobate.

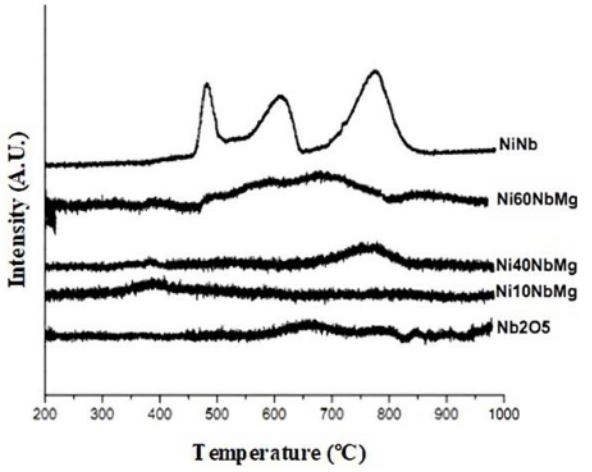

Fig. 2. Profiles obtained by H_2-TPR (Temperature Programmed Reduction with H_2) of analysis of the oxide catalysts.

On the other hand, as can be seen in the same Fig.2, NiMg, Ni10NbMg, and Ni40NbMg catalysts present a very low reduction, this is expected because these catalysts have NiO-MgO solid solution in their composition (as seen in XRD analyses). The conformation of this solid solution makes it difficult to reduce from Ni^{2+} to Ni°; in the case of the NiO-MgO solid solution the polarization of the Ni-O and Mg-O bonds are very weak, possibly because both cations (Ni^{2+} and Mg^{2+}) have very close electronegativity values (Ni^{2+} =1.367 e Mg^{2+}=1.234) [19].

The Ni40NbMg sample shows a small and broad reduction peak with a maximum intensity at 750°C indicating that the highest Nb_2O_5 contents favor the reduction of Ni^{2+} (to form Ni). This may be related to the formation of $NiNb_2O_6$ (seen in XRD analyses) which is of low thermal stability and is easier to reduce (as seen in the TPR profile of NiNb catalyst). In the Ni60NbMg sample, the broad reduction peak attributed to Ni^{2+} is more noticeable than in the Ni40NbMg sample; confirming the previous observation.

SEM analyses

Figures 3-7 show the images obtained by SEM analyses of the calcined catalysts, before catalytic tests. Fig. 3 shows the SEM image of the NiNb catalyst which, according to the XRD, is composed of nickel niobate. In this figure, a group of particles in the form of spherical grains that are agglomerated can be observed.

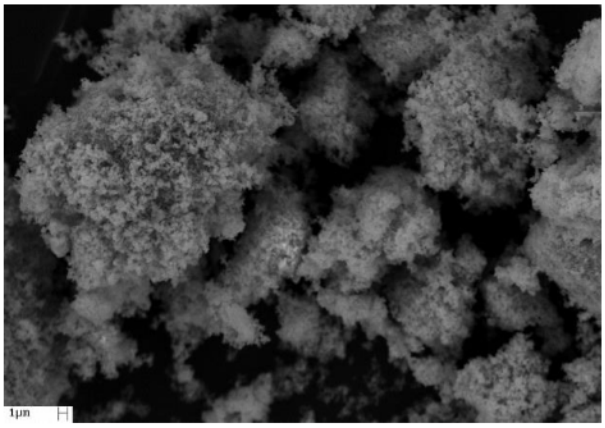

Figure 3. Image obtained by SEM analysis of the NiNb catalyst (x 5 000).

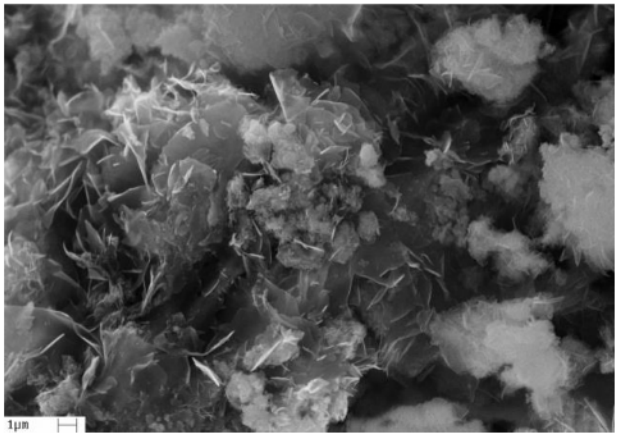

Figure 4. Image obtained by SEM analysis of the NiMg catalyst (x 10 000).

Fig.4 shows the image of NiMg sample, that is the NiO/MgO solid solution, at 10.000 amplifications; this image shows the formation of disorganized lamellar structures.

Figure 5 shows the morphology of the Ni10NbMg sample, it can be noted that the addition of 10% Nb_2O_5 in the NiO/MgO mixture noticeably modifies the morphology of the material compared to the NiMg sample (seen in Figure 4). This would indicate that the nickel niobate compound (which has the form of spherical grains as seen in Figure 3) would be covering the surface of the NiO-MgO solid solution, which forms lamellar structures (seen in Figure 4).

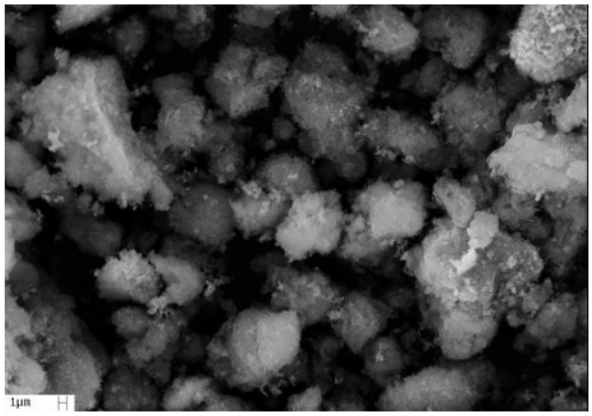

Figure 5. Image obtained by SEM analysis of the Ni10NbMg catalyst (x 5 000).

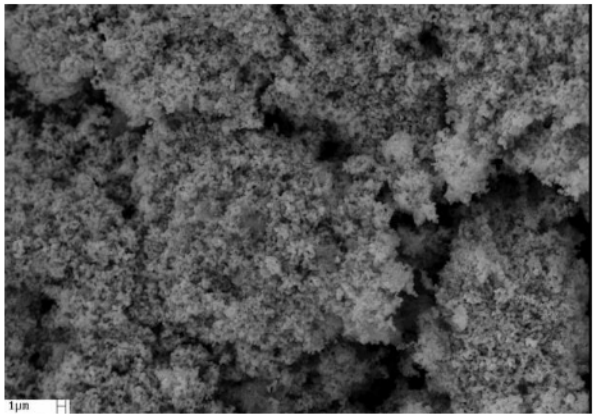

Figure 6. Images obtained by SEM analysis of Ni40NbMg catalyst (5 000x).

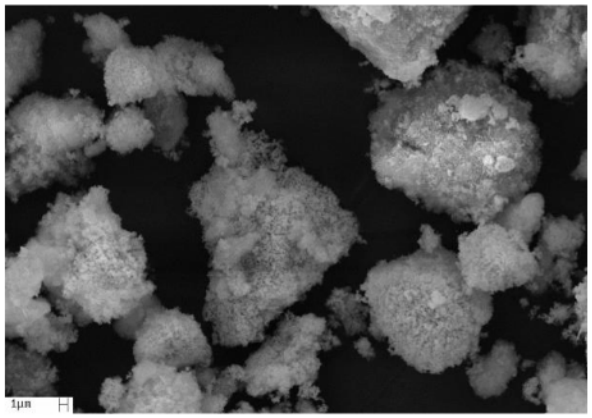

Figure 7. Images obtained by SEM analysis of Ni60NbMg catalyst (5000x).

Figures 6 and 7 are very similar to each other (Ni40NbMg and Ni60NbMg samples, respectively), as the surface of the catalysts is more populated with spherical agglomerates that correspond to nickel niobate because this structure would be covering the NiO-MgO solid solution (that forms lamellar structures, as observed in the image of Ni10NbMg).

Oxidative Reform of Biogas Reactions

The results of the catalytic test for the oxidative reform of the biogas (ORB) for T=750°C and a gaseous feed with molar ratios of CH_4:CO_2:O_2 = 1.5:1:0.25 are shown in Figures 8-10. According to these results, the highest conversion values of reactants (CH_4 and CO_2) were obtained using NiMg, Ni60NbMg, and Ni40NbMg catalysts. The CH_4 and CO_2 conversion (%) into Syngas (H_2/CO) decreased in the following order: NiMg≡Ni60NbMg>Ni40NbMg>Ni10NbMg>NiNb. In other words, the conversions of reactants increased with MgO content in the Nickel catalyst.

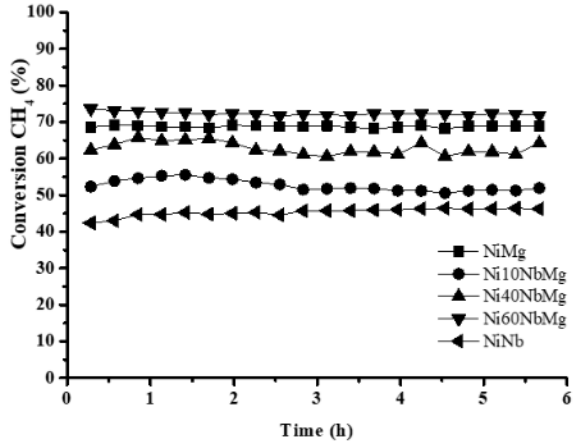

Figure 8. Methane conversion profile (CH_4) in the oxidative reforming of biogas on NiO-Nb_2O_5-MgO catalysts.

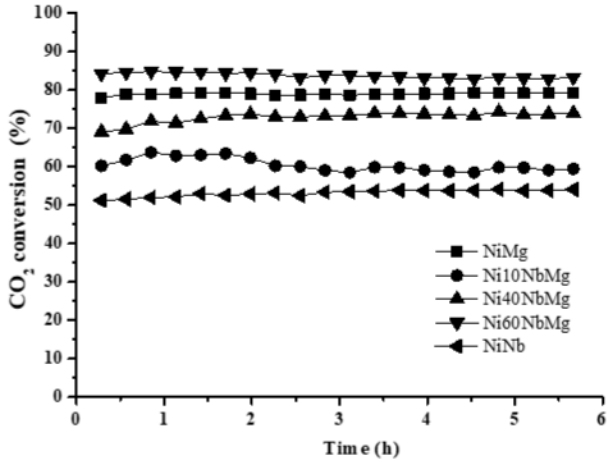

Figure 9. Carbon dioxide conversion (CO_2) in the oxidative reforming of biogas on NiO-Nb_2O_5-MgO catalysts.

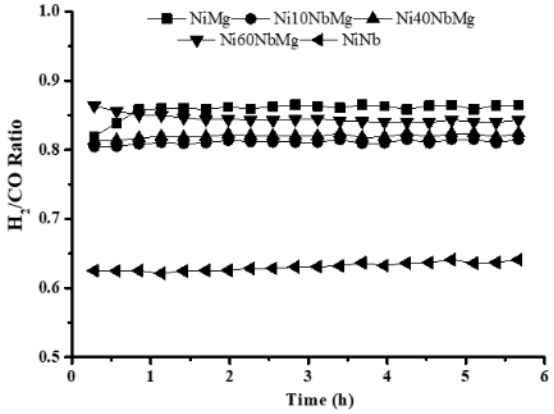

Figure 10. H_2/CO ratio in the products obtained during the oxidative reforming of biogas on NiO-Nb_2O_5-MgO catalysts.

There is no defined mechanism for how oxidative reform of methane (Reaction 1) occurs at a molecular level, however, previous studies [12], [21]–[24] state that this reaction occurs through DRM (Reaction 2) and POM (Reaction 3), each reaction following their respective known mechanisms:

DRM: $1.5CH_4 + CO_2 \rightarrow 2CO + 2H_2 + 0.5CH_4$
$\Delta H° = 260.5\ kJ.mol^{-1}$ (2)

POM: $0.5\ CH_4 + 0.25O_2 \rightarrow 0.5CO + H_2$
$\Delta H° = -22.6\ kJ.mol^{-1}$ (3)

Thus POM can occur by the direct mechanism, which involves the breakdown of the methane molecule to directly give H_2 and CO (Reaction 3); or by the indirect mechanism also known as total methane combustion-reforming that occurs through reactions 4-6, where the total sum of TCM + DRM + 2xSRM gives POM:

TCM: $CH_4 + 2O_2 \rightarrow CO_2 + 2H_2O$ $\Delta H° = -890\ kJ.mol^{-1}$ (4)
DRM: $CH_4 + CO_2 \rightarrow 2CO + 2H_2$ $\Delta H° = 260.5\ kJ.mol^{-1}$ (5)
SRM: $CH_4 + H_2O \rightarrow CO + 3H_2$ $\Delta H° = 225.4\ kJ.mol^{-1}$ (6)

On the other hand, to understand which steps the oxidative reforming of biogas goes through, we are going to consider the direct mechanism of POM reaction in the following paragraphs. In this case in POM reaction, the dissociation of the methane molecules occurs at the Ni° sites (small clusters of Ni°), which produces chemisorbed carbon atoms ($C_{(s)}$) on the surface of Ni° sites and chemisorbed hydrogen ($H_{(s)}$), and, on the other hand, oxygen molecules also dissociate on the surface of the catalyst giving chemisorbed oxygen ($O_{(s)}$), the following reactions (7-8) express these events:

$CH_4 + site \rightarrow C_{(s)} + 4H_{(s)}$ (7)
$O_{2(g)} + site \rightarrow 2\ O_{(s)}$ (8)
$C_{(s)} + O_{(s)} \rightarrow CO$ (9)
$C_{(s)} + CO_2 \leftrightarrow 2\ CO$ (10)
$H_{(s)} + H_{(s)} \rightarrow H_2$ (11)

Where "site" represents an active center on the surface of the catalyst. On the other hand, it can be seen in reaction (9) that the oxidation of coke to produce CO needs oxygen atoms, these can come from the breakdown of the O_2 molecules (reaction 8) as well as from CO_2 molecules (reaction 10). Reaction (11) is the one that gives the molecular hydrogen.

According to Kroll et al. [25], the DRM reaction involves reactions 12-14:

$CO_2 + C_{(s)} \rightarrow 2CO + site$ (12)
$CO_2 + site \rightarrow CO + O_{(s)}$ (13)
$C_{(s)} + O_{(s)} \rightarrow CO + 2\ site$ (14)

Catalysts must have adequate properties to activate CO_2 and O_2 molecules; for instance, some solid solutions based on ZrO_2 have excellent properties to activate CO_2 and O_2 during methane reforming and partial oxidation of methane reactions [5]. In the case of NiO-MgO-Nb_2O_5 catalysts, MgO may be favoring the activation of CO_2, as previously reported in [26], [27] for NiO-ZrO_2 catalyst in Dry reforming of methane.

The coke deposition rates reported for each catalyst during the oxidative reforming of biogas were: NiMg (0.28 $mmolC.h^{-1}$), Ni10NbMg (0.52 $mmolC.h^{-1}$), Ni40NbMg (0.33 $mmolC.h^{-1}$), Ni60NbMg (0.35 $mmolC.h^{-1}$) e NiNb (0.65 $mmolC.h^{-1}$). In parallel, the values for the rate of water produced during the oxidative reforming of biogas (collected as a by-product), were: NiMg (11 $mmolH_2O.h^{-1}$), Ni10NbMg (11 $mmolH_2O.h^{-1}$), Ni40NbMg (9 $mmolH_2O.h^{-1}$), Ni60NbMg (9 $mmolH_2O.h^{-1}$) e NiNb (19 $mmolH_2O.h^{-1}$).

The Ni60NbMg catalyst was the best catalyst for the oxidative reforming of biogas because, over it, the reaction recorded high reactant conversion values (see Figures 8 and 9) and a relatively low coke deposition rate. Despite the reactant conversion over NiMg being very close to that obtained over Ni60NbMg, and its carbon deposition value being slightly lower than that obtained by Ni60NbMg, the NiMg catalyst was not considered the best catalyst. This is because the composition of the NiMg catalyst, that is the NiO/MgO solid solution, widely studied [13], [14], [28]–[31], it presents problems in scale-up studies, due to the low mechanical strength of MgO and its hygroscopic character. At this point, it is very important to consider that the objective of this work is to find alternative catalysts to the commercial Ni/Al_2O_3.

Traces of water were collected at the end of each catalytic test, this could be related to the occurrence of the reverse of water-gas shift reaction (RWGSR), expressed in the reaction (15). The occurrence of RWGSR may explain why the CO_2 conversion is slightly higher than the CH_4 conversion (see Figures 8 and 9):

RWGSR: $CO_2 + H_2 \leftrightarrow CO + H_2O$ $\Delta H° = 34.3\ kJ.mol^{-1}$ (15)

Figure 11 shows the values of the H_2/CO ratio in the products obtained during the oxidative reforming of biogas. The H_2/CO ratios were always lower than 1.2 (stoichiometric value given in reaction 1), this can be explained due to the consumption of

hydrogen by the RWGSR (Reaction 15). The values of the H_2/CO ratio obtained over NiMg and Ni60NbMg catalysts were the closest to the stoichiometric value.

Taking into account the results obtained in the catalytic tests and the characterization of the catalysts, it is possible to affirm that the catalysts containing the three oxides with the highest presence of $NiNb_2O_6$ favored the conversion of CH_4 and CO_2, as the conversion % of reactants decreased as follows: Ni60NbMg>Ni40NbMg >Ni10NbMg. On the other hand, the NiNb catalyst whose predominance is the $NiNb_2O_6$ compound, obtained a low catalytic performance in the oxidative reform of biogas reaction, which demonstrates that the $NiNb_2O_6$ compound is only effective when MgO is present in the catalyst. This suggests that there is a synergistic effect between $NiNb_2O_6$ and NiO-MgO in the NiO-MgO-Nb_2O_5 catalysts.

As discussed previously, the formation of $NiNb_2O_6$ becomes interesting because its reduction with H_2 (during activation before the catalytic reaction) leads to a strong metal-support interaction (Ni^o/Nb_2O_5), which is important to obtain good catalytic activity [32]. Also, the reduction of $NiNb_2O_6$ with H_2 leads to a high dispersion of Ni° that favors the decomposition of methane by breaking the C-H bonds [16]. Wojcieszak et al.[33] carried out a study of catalysts based on NiO/Nb_2O_5 and reported two important facts: there is a strong interaction of Ni and Nb_2O_5 in the NiO/Nb_2O_5 catalyst, and the strong acidity of Nb_2O_5 is increased by the incorporation of NiO in the mixture. In this context, the low catalytic performance of the NiNb catalyst denoted in the present study may be related to its high acidity, which leads to high carbon formation (according to our experiment: 0.65 $mmol.C.h^{-1}$). In this sense, the NiNb catalyst seems to have more active centers for the dissociation of the CH_4 molecules than active centers for the activation of the O_2 and CO_2 molecules; as seen in reaction (12), the dissociation of CO_2 helps to remove the chemisorbed carbon on the catalyst surface.

It is known that the addition of alkaline oxides to catalysts supported on alumina or silica can favor the activation of CO_2 molecules during Dry Reforming of Methane (DRM, reaction 5), due to the decrease of acid sites of the catalyst [34]. According to Bitter et al.[35], Bitter et al.[36], and Wei et al. [37] the addition of MgO to catalytic supports of Nickel catalysts improves the activation of CO_2 molecules during DRM through the formation of carbonate species at the metal-support interface, which is subsequently reduced by the deposited carbon, producing formate (an intermediate product) that is subsequently decomposed into CO.

Furthermore, taking into account that CO_2 is an acidic molecule, CO_2 molecules can react more easily with MgO basic centers of the $NiO/Nb_2O_5/MgO$ catalyst synthesized in the present work, an acid-base interaction would favor this reaction [38]. These observations could reinforce the explanation of why the trend found in the catalytic tests was:
NiMg>Ni60NbMg>Ni40NbMg>Ni10NbMg>NiNb.
According to this, is clear that the largest presence of MgO increased the CH_4 and CO_2 conversion % values.

The catalytic test results demonstrated that the composition of the Ni60NbMg catalyst is optimal to achieve good catalytic performance in the oxidative reform of biogas; part of the acidity of $NiNb_2O_6$ would be neutralized by the addition of MgO, which also gives rise to the NiO-MgO solid solution. Active centers for activation of CH_4 and CO_2 molecules would be in optimal quantities in the Ni60NbMg catalyst.

Characterization of catalysts after the oxidative reform of biogas.

Although the mechanism of coke formation in methane reforming and partial oxidation reactions is not clearly understood, its formation over nickel catalysts is inevitable. Some studies [39], [40] claim that the mechanism of coke formation starts with the dissociation of the methane molecule to produce highly reactive chemisorbed carbon atoms (C_α) on the surface. This carbon is easily gasified, but if the gasification is slow, it polymerizes, forming C_β carbon which diffuses through the active metal (Ni° in this case), forming filaments.

Figures 11 and 12 show the images obtained by the scanning electron microscope (SEM) of the wasted catalysts Ni60NbMg and NiMg, respectively, after 6 hours of oxidative reform of biogas. In these figures, it is observed that the catalysts form filamentous carbon. As expected, the morphology of these filaments changes from one catalyst to another; the filaments are thicker and more defined in the NiMg catalyst (Fig. 12); whereas in the Ni60NbMg catalyst (Fig. 11), the filaments are much thinner. The image of the coke formed by Ni10NbMg and Ni40NbMg are practically the same as Ni60NbMg (this is why they were not shown in this manuscript). The results obtained in catalytic tests indicated that this type of coke did not affect the stability of the catalyst in the oxidative reform of biogas.

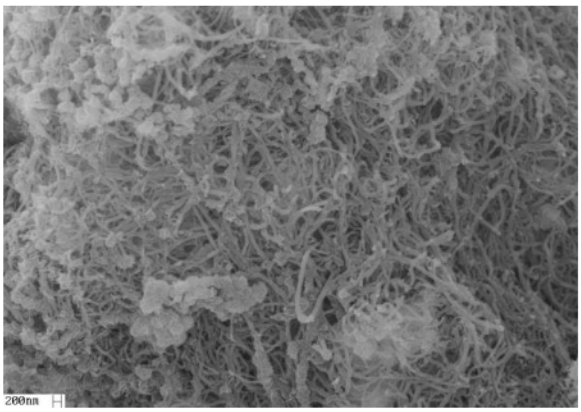

Figure 11. SEM images obtained from the Ni60NbMg catalyst after 6 hours of reaction.

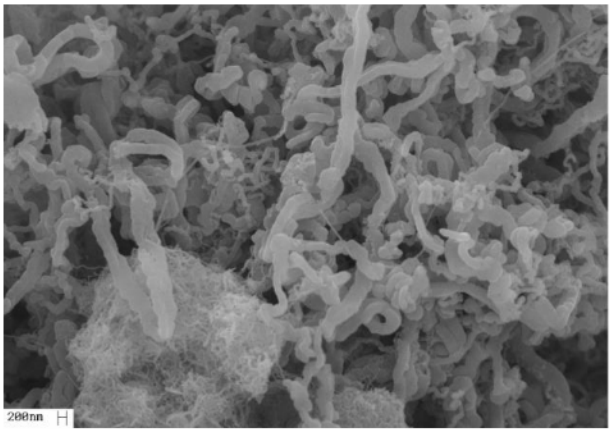

Figure 12. SEM images obtained from the NiMg catalyst after 6 hours of reaction.

IV. Conclusion

The addition of MgO in the NiO/Nb_2O_5 catalyst improved the performance of catalysts in the oxidative reform of biogas. The catalyst with 60% Nb_2O_5 presented the highest conversion value, and presented a relatively low amount of coke deposition rate, showing as promising for the oxidation reform of biogas.

XRD and TPR analyses confirmed the formation of NiO-MgO solid solutions and the formation of nickel niobate ($NiNb_2O_6$) in the catalysts. These compounds together had a synergy that improved the performance of Ni-MgO-Nb_2O_5 catalysts during the oxidative reform of biogas.

Pure nickel niobate ($NiNb_2O_6$) did not show good catalytic activity, this could be related to its high acidity which led to a high rate of coke formation.

During the oxidative reform of biogas, these catalysts formed filamentous carbon that did not affect the stability of the catalyst during the reaction time.

Acknowledgment

Thanks to Companhia Brasileira de Metalurgia e Mineração (Portuguese for Brazilian Metallurgy and Mining Company) for the Niobium provided for the preparation of the catalysts, and thanks to the São Carlos Institute of Chemistry of Universidade de São Paulo (USP), for the facilities for this study.

References

[1] E. Winquist, P. Rikkonen, J. Pyysiäinen, and V. Varho, "Is biogas an energy or a sustainability product? - Business opportunities in the Finnish biogas branch," *J Clean Prod*, vol. 233, 2019, doi: 10.1016/j.jclepro.2019.06.181.

[2] Y. J. O. Asencios, C. B. Rodella, and E. M. Assaf, "Biomethane reforming over Ni catalysts supported on PrO2-ZrO2 solid-solutions," *Journal of CO2 Utilization*, vol. 61, p. 102018, Jul. 2022, doi: 10.1016/j.jcou.2022.102018.

[3] I. A. Cruz *et al.*, "Valorization of cassava residues for biogas production in Brazil based on the circular economy: An updated and comprehensive review," *Cleaner Engineering and Technology*, vol. 4. 2021. doi: 10.1016/j.clet.2021.100196.

[4] Y. J. O. Asencios, K. F. M. Elias, and E. M. Assaf, "Oxidative-reforming of model biogas over NiO/Al <inf>2</inf> O <inf>3</inf> catalysts: The influence of the variation of support synthesis conditions," *Appl Surf Sci*, vol. 317, 2014, doi: 10.1016/j.apsusc.2014.08.058.

[5] Y. J. O. Asencios *et al.*, "Partial Oxidation of Biomethane over Nickel Supported on MgO–ZrO2 Solid Solutions," *Top Catal*, 2023, doi: 10.1007/s11244-023-01822-7.

[6] A. L. D. Ramos, J. J. Marques, V. Dos Santos, L. D. S. Freitas, R. G. V. De Melo Santos, and M. De Mattos Vieira Mello Souza, "Atual estágio de desenvolvimento da tecnologia gtl e perspectivas para o Brasil," *Quim Nova*, vol. 34, no. 10, 2011, doi: 10.1590/s0100-40422011001000004.

[7] Y. J. O. Asencios, J. D. A. Bellido, and E. M. Assaf, "Synthesis of NiO-MgO-ZrO<inf>2</inf> catalysts and their performance in reforming of model biogas," *Appl Catal A Gen*, vol. 397, no. 1–2, 2011, doi: 10.1016/j.apcata.2011.02.023.

[8] Y. J. O. Asencios and E. M. Assaf, "Combination of dry reforming and partial oxidation of methane on NiO-MgO-ZrO<inf>2</inf> catalyst: Effect of nickel content," *Fuel Processing Technology*, vol. 106, 2013, doi: 10.1016/j.fuproc.2012.08.004.

[9] Y. J. O. Asencios and E. M. Assaf, "Combination of dry reforming and partial oxidation of methane on NiO-MgO-ZrO2 catalyst: Effect of nickel content," *Fuel Processing Technology*, vol. 106, 2013, doi: 10.1016/j.fuproc.2012.08.004.

[10] Y. J. O. Asencios, P. A. P. Nascente, and E. M. Assaf, "Partial oxidation of methane on NiO-MgO-ZrO <inf>2</inf> catalysts," *Fuel*, vol. 97, 2012, doi: 10.1016/j.fuel.2012.02.067.

[11] G. Y. Boyarko, "Dynamics of global production and commodity flows of niobium raw materials," *Bulletin of the Tomsk Polytechnic University, Geo Assets Engineering*, vol. 330, no. 10, 2019, doi: 10.18799/24131830/2019/10/2318.

[12] V. R. Choudhary and A. S. Mamman, "Energy efficient conversion of methane to syngas over NiO-MgO solid solution," *Appl Energy*, vol. 66, no. 2, 2000, doi: 10.1016/S0306-2619(99)00039-2.

[13] E. Ruckenstein, "Binary MgO-based solid solution catalysts for methane conversion to syngas," *Catal Rev Sci Eng*, vol. 44, no. 3, 2002, doi: 10.1081/CR-120005742.

[14] Y. H. Hu and E. Ruckenstein, "The characterization of a highly effective NiO / MgO solid solution catalyst in the CO2 reforming of CH4," *Catal Letters*, vol. 43, no. 1–2, 1997, doi: 10.1023/a:1018982304573.

[15] R. D. Shannon, "Revised effective ionic radii and systematic studies of interatomic distances in halides and chalcogenides," *Acta Crystallographica Section*

A, vol. 32, no. 5, 1976, doi: 10.1107/S0567739476001551.

[16] K. Kunimori, H. Oyanagi, and H. Shindo, "Nickel-niobia interaction induced by the reduction of NiNb2O6 supported on SiO2," *Catal Letters*, vol. 21, no. 3–4, 1993, doi: 10.1007/BF00769480.

[17] L. Guochang, L. Peraldo Bicelli, G. Razzini, and R. Borromei, "Surface investigation of NiNb2O6 electrodes for water photoelectrolysis," *Mater Chem Phys*, vol. 23, no. 5, 1989, doi: 10.1016/0254-0584(89)90091-6.

[18] A. Martínez-De La Cruz, N. L. Alcaraz, A. F. Fuentes, and L. M. Torres-Martínez, "Electrochemical lithium insertion in some niobates MNb2O6 (M = Mn, Co, Ni, Cu, Zn and Cd)," *J Power Sources*, vol. 81–82, 1999, doi: 10.1016/S0378-7753(99)00198-6.

[19] K. Li and D. Xue, "Estimation of electronegativity values of elements in different valence states," *Journal of Physical Chemistry A*, vol. 110, no. 39, 2006, doi: 10.1021/jp062886k.

[20] A. C. Faro, P. Grange, and A. C. B. dos Santos, "Niobia-supported nickel-molybdenum catalysts: Characterisation of the oxide form," *Physical Chemistry Chemical Physics*, vol. 4, no. 16, 2002, doi: 10.1039/b202517e.

[21] T. V. Choudhary and V. R. Choudhary, "Energy-efficient syngas production through catalytic oxy-methane reforming reactions," *Angewandte Chemie - International Edition*, vol. 47, no. 10. 2008. doi: 10.1002/anie.200701237.

[22] V. R. Choudhary, K. C. Mondal, and T. V. Choudhary, "Oxy-CO2 reforming of methane to syngas over CoOx/MgO/SA-5205 catalyst," *Fuel*, vol. 85, no. 17–18, 2006, doi: 10.1016/j.fuel.2006.04.013.

[23] V. R. Choudhary and A. S. Mamman, "Oxidative conversion of methane to syngas over NiO/MgO solid solution supported on low surface area catalyst carrier," *Fuel Processing Technology*, vol. 60, no. 3, 1999, doi: 10.1016/S0378-3820(99)00046-6.

[24] V. R. Choudhary, B. S. Uphade, and A. S. Mamman, "Simultaneous steam and CO2 reforming of methane to syngas over NiO/MgO/SA-5205 in presence and absence of oxygen," *Appl Catal A Gen*, vol. 168, no. 1, 1998, doi: 10.1016/S0926-860X(97)00331-1.

[25] V. C. H. Kroll, H. M. Swaan, S. Lacombe, and C. Mirodatos, "Methane reforming reaction with carbon dioxide over Ni/SiO2 catalyst: II. A mechanistic study," *J Catal*, vol. 164, no. 2, 1996, doi: 10.1006/jcat.1996.0395.

[26] J. D. A. Bellido and E. M. Assaf, "Effect of the Y2O3-ZrO2 support composition on nickel catalyst evaluated in dry reforming of methane," *Appl Catal A Gen*, vol. 352, no. 1–2, 2009, doi: 10.1016/j.apcata.2008.10.002.

[27] J. D. A. Bellido, J. E. De Souza, J. C. M'Peko, and E. M. Assaf, "Effect of adding CaO to ZrO2 support on nickel catalyst activity in dry reforming of methane," *Appl Catal A Gen*, vol. 358, no. 2, 2009, doi: 10.1016/j.apcata.2009.02.014.

[28] E. Ruckenstein and Y. H. Hu, "Carbon dioxide reforming of methane over nickel/alkaline earth metal oxide catalysts," *Appl Catal A Gen*, vol. 133, no. 1, 1995, doi: 10.1016/0926-860X(95)00201-4.

[29] E. Ruckenstein and Y. H. Hu, "Methane partial oxidation over NiO/MgO solid solution catalysts," *Appl Catal A Gen*, vol. 183, no. 1, 1999, doi: 10.1016/S0926-860X(99)00047-2.

[30] Y. H. Hu and E. Ruckenstein, "An optimum NiO content in the CO2 reforming of CH4 with NiO/MgO solid solution catalysts," *Catal Letters*, vol. 36, no. 3–4, 1996, doi: 10.1007/BF00807611.

[31] Y. H. Hu and E. Ruckenstein, "Catalyst temperature oscillations during partial oxidation of methane," *Ind Eng Chem Res*, vol. 37, no. 6, 1998, doi: 10.1021/ie980027f.

[32] C. E. M. Guarido, D. V. Cesar, M. M. V. M. Souza, and M. Schmal, "Ethanol reforming and partial oxidation with Cu/Nb2O5 catalyst," *Catal Today*, vol. 142, no. 3–4, 2009, doi: 10.1016/j.cattod.2008.08.030.

[33] R. Wojcieszak, A. Jasik, S. Monteverdi, M. Ziolek, and M. M. Bettahar, "Nickel niobia interaction in non-classical Ni/Nb2O5 catalysts," *J Mol Catal A Chem*, vol. 256, no. 1–2, 2006, doi: 10.1016/j.molcata.2006.04.053.

[34] A. Guerrero-Ruiz, A. Sepúlveda-Escribano, and I. Rodríguez-Ramos, "Cooperative action of cobalt and MgO for the catalysed reforming of CH4 with CO2," *Catal Today*, vol. 21, no. 2–3, 1994, doi: 10.1016/0920-5861(94)80178-9.

[35] J. H. Bitter, K. Seshan, and J. A. Lercher, "The state of zirconia supported platinum catalysts for CO2/CH4 reforming," *J Catal*, vol. 171, no. 1, 1997, doi: 10.1006/jcat.1997.1792.

[36] J. H. Bitter, K. Seshan, and J. A. Lercher, "Mono and bifunctional pathways of CO2/CH4 reforming over Pt and Rh based catalysts," *J Catal*, vol. 176, no. 1, 1998, doi: 10.1006/jcat.1998.2022.

[37] J. M. Wei, B. Q. Xu, J. L. Li, Z. X. Cheng, and Q. M. Zhu, "Highly active and stable Ni/ZrO2 catalyst for syngas production by CO2 reforming of methane," *Appl Catal A Gen*, vol. 196, no. 2, 2000, doi: 10.1016/S0926-860X(99)00504-9.

[38] Z. Hou, O. Yokota, T. Tanaka, and T. Yashima, "A novel KCaNi/α-Al2O3 catalyst for CH 4 reforming with CO2," *Catal Letters*, vol. 87, no. 1–2, 2003, doi: 10.1023/A:1022849009431.

[39] V. V. Chesnokov, V. I. Zaikovskii, R. A. Buyanov, V. V. Molchanov, and L. M. Plyasova, "Morphology of carbon from methane on nickel-containing catalysts," *Catal Today*, vol. 24, no. 3, 1995, doi: 10.1016/0920-5861(95)00040-M.

[40] J. W. Snoeck, G. F. Froment, and M. Fowles, "Filamentous carbon formation and gasification: Thermodynamics, driving force, nucleation, and steady-state growth," *J Catal*, vol. 169, no. 1, 1997, doi: 10.1006/jcat.1997.1634.